Universal Library of Engineering Technology Research Article

ISSN: 3064-996X | Volume 1, Issue 1

Open Access | PP: 41-49

DOI: https://doi.org/10.70315/uloap.ulete.2024.0101006

Brine Salinity: A Deciding Factor for Carbondioxide Dissolution and Trapping during Geological Sequestration

Bright Bariakpoa Kinate*, Seth Uba Wadike, Godloves Tondie Nonju, Nyelebuchi Amadichuku

Department of Petroleum Engineering, Rivers State University, Nigeria.

Abstract

Adequate geological storage of carbondioxide in saline aquifers is a function of several factors that requires understanding and examination. Previous works have argue that solubility of carbondioxide in brine decreases as the salinity of the brine increases, but it is unclear in the literature the impact of salinity on carbondioxide (CO_2) trapping during sequestration. This work adopt a simulation based approach to determine CO_2 dissolution and trapping at different salinities. A dataset was written and validated with CMG's greenhouse gases simulator and the thermodynamics properties calculation carried out with Peng-Robinson equation of state. Four sensitivity analyses was conducted with brines of no salinity (pure water), salinity of 100000ppm, 200000ppm and 300000ppm and model outputs compared for CO_2 sequestration. The result shows that CO_2 solubilised in water with zero level salinity, and a lower gas cap size was formed at the top of the structure. Later, gas cap size increases as the salinity level increases at the top of the structure. Also, the moles soluble in water decreases as the salinity level increases with the least moles for zero water salinity. Alternatively to the moles solubilised, the number of moles of CO_2 trapped increases with the salinity level. CO_2 storage in deep saline aquifers is the best storage techniques but its injection into aquifer of high salinity reduced its solubility.

Keywords: *Brine Salinity, CO_2 Dissolved, CO_2 Trapped, Sequestration, Solubilized.*

INTRODUCTION

Carbondioxide(CO_2) having its main source from burning of fossil fuels has continuously increase concentration of greenhouse gas in the atmosphere and require control to reduce global warming and environmental issues(Xie and Economides, 2009; Ahmadi *et al.,* 2016). So many approach have been studied and investigated to reduce the emission of CO_2 to the atmosphere so as to control global warming to an extent (Mathieu, 2006). Among these notable approach and measures, CO_2 sequestration has prove to be a promising strategy to reduce carbon emissions. CO_2 sequestration is the only storage method that reduces the concentration of CO_2 in the atmosphere without affecting the fossil fuels consumption level, and it is becoming popular and the most recommended for safety of the environment (Leung *et al.,* 2014). Geological sequestration entails storing captured CO_2 in deep geologic formations such as saline aquifers, and basalt formations (Shukla *et al.,* 2010; Otheim *et al.,* 2011).

CO_2 sequestration has been quantified as dependent on the rate of CO_2 dissolution into brines and their migration dynamics. The accumulation of CO_2 is a function of molecular diffusion before it dissolves in to formation brine. Consequently, the density of the brine increases with CO_2 dissolution, resulting to a phase segregation of the denser brine, and eventually leads to natural convective mixing driven by the density distinction from formation brines (Nordbotten *et al.,* 2005). Previous works have shown that convective mixing is affected not only by a porous medium's porosity, permeability, and thickness, but also by mineralization of brine and its initial density (Agartan *et al.,* 2015; Taheri *et al.,* 2021; Amarasinghe *et al.,* 2021; Faisal *et al.,* 2003).

The underlying factors that influenced carbondioxide trapping and dissolution is still controversial and not fully explored even with few experimental and numerically analysis on injection and transport of CO_2 in saline aquifers conditions (Chalbaud *et al.,* 2009, Alkan *et al.,* 2010, Al-Khdheeawi *et al.,* 2018;). Another study shows that increase in relative permeability hysteresis increases the CO_2 trapped (Amadichuku et al.,2023). Past works have opined that solubility of CO_2 in brine decreases as the salinity of the brine increases (Yan *et al.,* 2011;De Silva *et al.,* 2015; Zhao *et al.,* 2015; Ahmadi and Chapoy, 2018). However, it is not yet clear how salinity increases or decreases carbondioxide trapping and dissolution during sequestration.

Therefore, this work investigates the influenced of brine salinity on carbondioxide trapping and dissolution during saline aquifer storage.

METHODOLOGY

Computer Modelling Group (CMG) simulator and Grid properties, fluid model creation, brine properties, water and gas relative permeability ,and model initiation data presented in Table 1 to Table 6 were used in this work.

Table 1. Grid properties data

Properties	Value
Grid Top	1200m
Grid thickness	5m
Permeability (I, J and K)	100 millidarcies
Porosity	0.12
Rock compressibility	5.5e-7 per kPa
Reference pressure for rock compressibility	11800 kPa

Table 2. Data for GEM fluid model creation

Component	Mole fraction
CH_4	0.999
CO_2	0.001
Reservoir temperature for GEM fluid model	50°C

Table 3. Brine properties

Property	Value
Water density	1020kg/m^3
Water compressibility	4.35e-7 per psi
Reference pressure	11800kPa

Table 4. Water relative permeability data

Sw	krw	krow
0.2	0	1
0.2899	0.0022	0.6769
0.3778	0.018	0.4153
0.4667	0.0607	0.2178
0.5558	0.1438	0.0835
0.6444	0.2809	0.0123
0.7	0.4089	0
0.7333	0.4855	0
0.8222	0.7709	0
0.9111	0.95	0
1	0.9999	0

Table 5. Gas relative permeability data

Sg	krg	krog
0.0006	0	1
0.05	0	0.88
0.0889	0.001	0.7023
0.1778	0.01	0.4705
0.2667	0.03	0.2963
0.3556	0.05	0.1715
0.4444	0.1	0.0878
0.5333	0.2	0.037
0.6222	0.35	0.011
0.65	0.39	0
0.7111	0.56	0
0.8	0.9999	0

Table 6. Model initialization data

Properties	Value
Temperature	50°C
Reference pressure	11800 kPa
Datum depth	1200m
Water gas contact	1150m
CO_2 fraction	0.001
CH_4	0.999

Builder was used in writing the dataset and validated with GEM. A two-dimensional (2D) homogeneous aquifer model of dimensions 100x1x20 (2000 grid blocks) was built with the data and the model was populated with petrophysical, grid and rock properties using the data in Table 1 and Table 2. Peng-Robinson 1978 equation of state was selected as for thermodynamic properties calculation. The CH_4 component was treated as the trace component. Li-Nghiem's model was used for the calculation of Henry's constant for gas solubility in brine. The created fluid model was imported into the component section of GEM data file. Data in Table 3 were used in defining the brine properties. Relative permeability data in Table 4 and Table 5 were used to define the relative permeability curves and the model was initialized using the data in Table 6. Water-Gas contact was set at 1150m above the reference depth which gave a model fully saturated with brine. Gas cap was initialized with supercritical CO_2 fraction of 0.001 and CH_4 fraction of 0.999 respectively. An injector well 'CO_2_INJECTOR' was completed in three layers at the bottom of the model at 1298m, 1299m and 1300m. The injector was shut-in after 5years of CO_2 injection, with only natural gradient driving the flow for 195years. After the base model (zero salinity level), three models with similar rock and fluid characteristics were simulated for different salinity of 100000ppm, 200000ppm, and 300000ppm.The simulation workflow is shown in Figure 1.

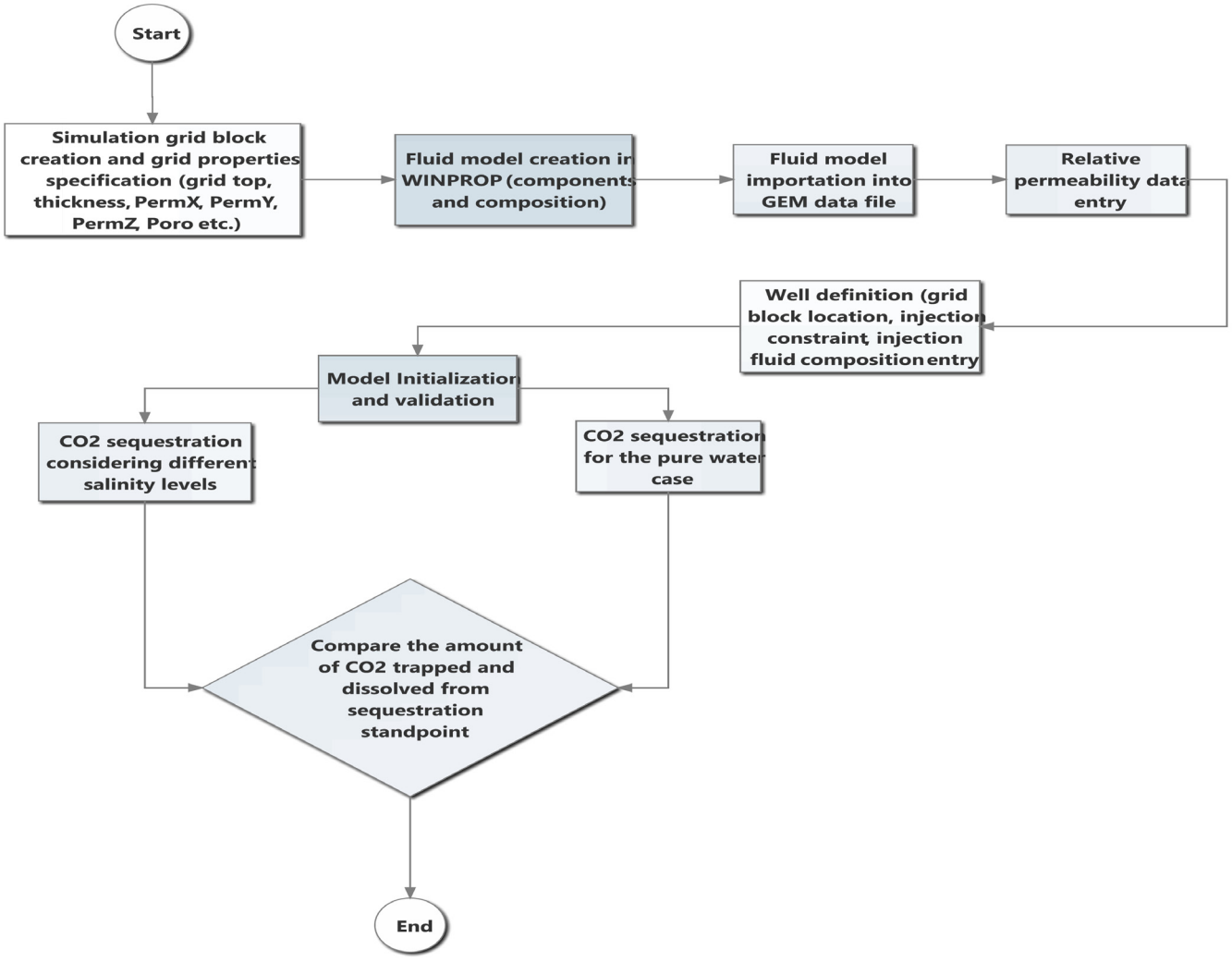

Figure 1. Simulation workflow

RESULTS AND DISCUSSION

CO_2 Dissolved and Trapped in Zero Salinity Level

The spatial distribution of CO_2 plume in saline aquifer for the base model is shown in figure 2. The base model shows the injection of CO_2 for 5years and the migration of the CO_2 plume during the next 195 years in aquifer with zero water salinity. The injected CO_2 migrated laterally during injection under the influence of pressure provided by the injection well. Post-injection, the lateral expansion of the plume ceased and CO_2 migrate upward due to its lighter density compare to formation water. There was a greater amount of CO_2 at the bottom of the structure due to the onset of solubility trapping mechanism. A gas cap of size 294.945m was formed at the top of the structure with CO2 soluble in zero salinity level

Figure 2. CO_2 spatial distribution for zero water salinity (pure water)

The amount of CO_2 trapped structurally and dissolved in brine during the injection period and post-injection period for zero water salinity level is presented in figure 3.During the injection period, 17631590moles of CO_2 were trapped structurally. For the Post-injection phase, the amount of CO_2 trapped structurally increases slightly and later decline after which it was constant at 16853558moles due to the onset of CO_2 solubility trapping. During the injection phase, 17991720moles of CO_2 was soluble in water while during the post-injection period, CO_2 solubility trapping gave 38286492moles of CO_2 in water.

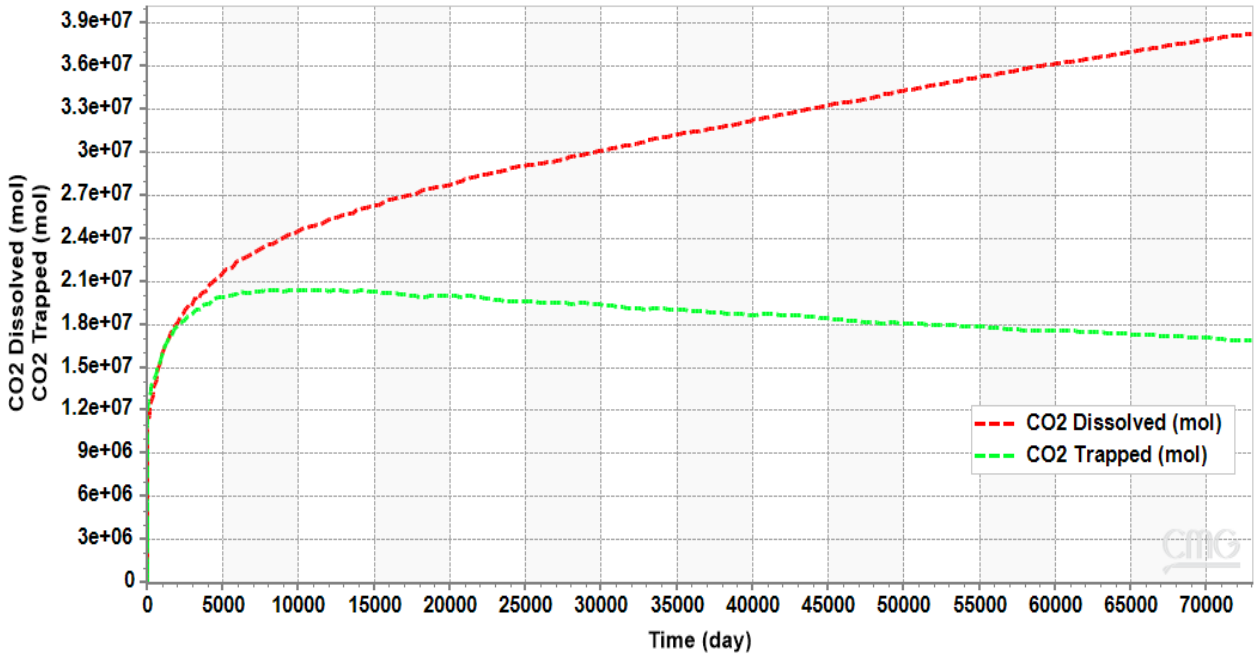

Figure 3. CO_2 trapped and dissolved for zero water salinity level (pure water)

CO_2 Dissolved and Trapped in 100000ppm Water

The 2D visualization of CO_2 plume migration in saline aquifer of water salinity 100000ppm is shown in figure 4. The model simulates the injection of CO_2 for 5years and its migration under natural buoyancy during the next 195years. The injected CO_2 migrate laterally during the injection phase under the influence of pressure provided by the injection well. After 195years, there was formation of gas cap of size 384.4325m in length and mobile supercritical CO_2 at the top of the formation with a saturation of 0.99.

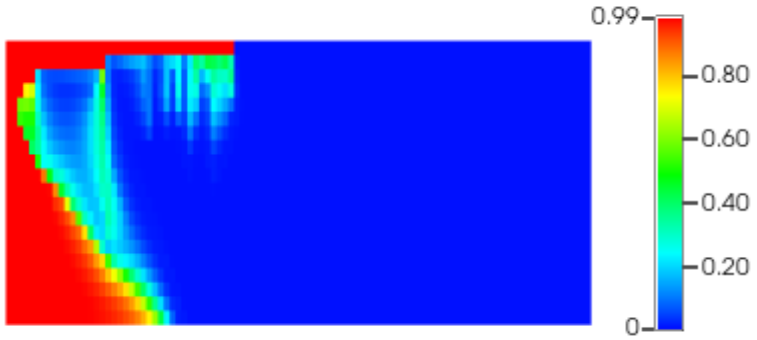

Figure 4. CO_2 spatial distribution for water salinity of 100000ppm

The amount of CO_2 trapped structurally during the injection period and post-injection period for 100000ppm water salinity level is presented in figure 5. During the injection period, 11132027 moles of CO_2 were trapped structurally while for the Post-injection phase, the amount of CO_2 trapped structurally increase slightly before maintaining 10693296 moles due to the onset of CO_2 solubility trapping .During the injection phase, 7566161.5moles of CO_2 was soluble in water and 16974034moles of CO_2 during the post-injection period.

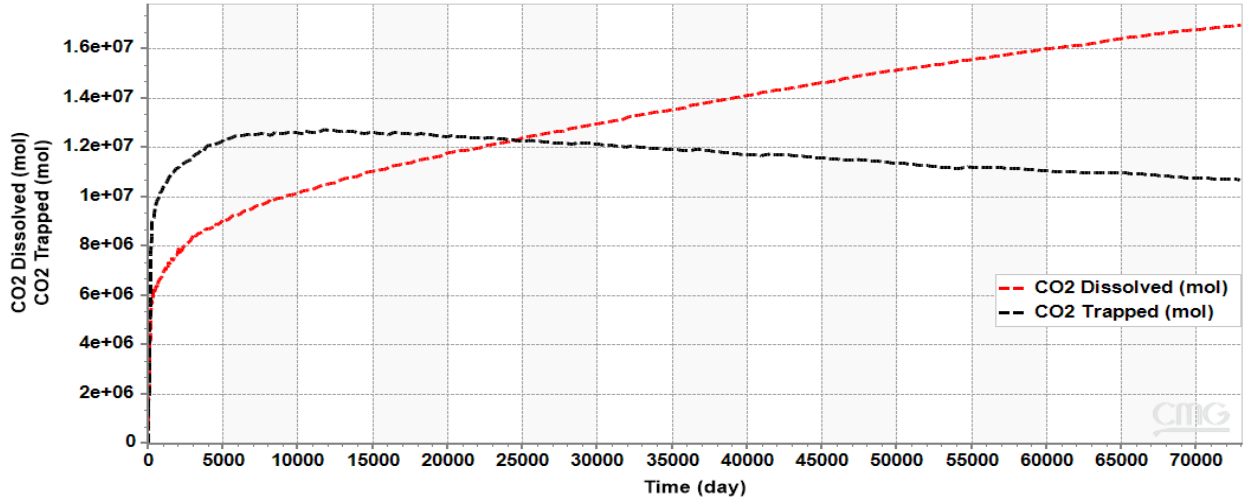

Figure 5. CO_2 trapped and dissolved for 100000ppm water salinity level

CO_2 Dissolved and Trapped in 200000ppm Water

Figure 6 shows the 2D visualization of CO_2 plume migration in saline aquifer of water salinity 200000ppm. After 195years, there was a formation of gas cap of mobile supercritical CO_2 at the top of the formation with a saturation of 0.99. With the CO_2 injector shut-in after 5years and CO_2 plume migration occurring under natural buoyancy during 195years, a gas cap of size 455.5605m was formed at the top of the structure.

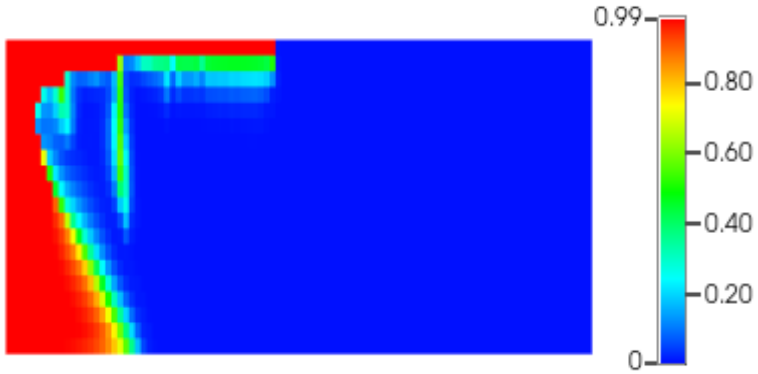

Figure 6. CO_2 spatial distribution for 200000ppm water salinity

The amount of CO_2 trapped for 200000ppm water salinity level is shown in figure 7. There was an increase in the amount of CO_2 trapped because of the influence of pressure provided by the injection well. For the Post-injection period, the amount of CO_2 trapped structurally reduced followed by the onset of solubility. For the injection period, 11587398moles of CO_2 were trapped structurally. The amount of CO_2 trapped structurally increases before maintaining 13000772 moles due to the

onset of CO_2 solubility for post injection phase. During the injection phase, 4560236moles of CO_2 was soluble in brine and 9807470moles of CO_2 in water for the post injection period.

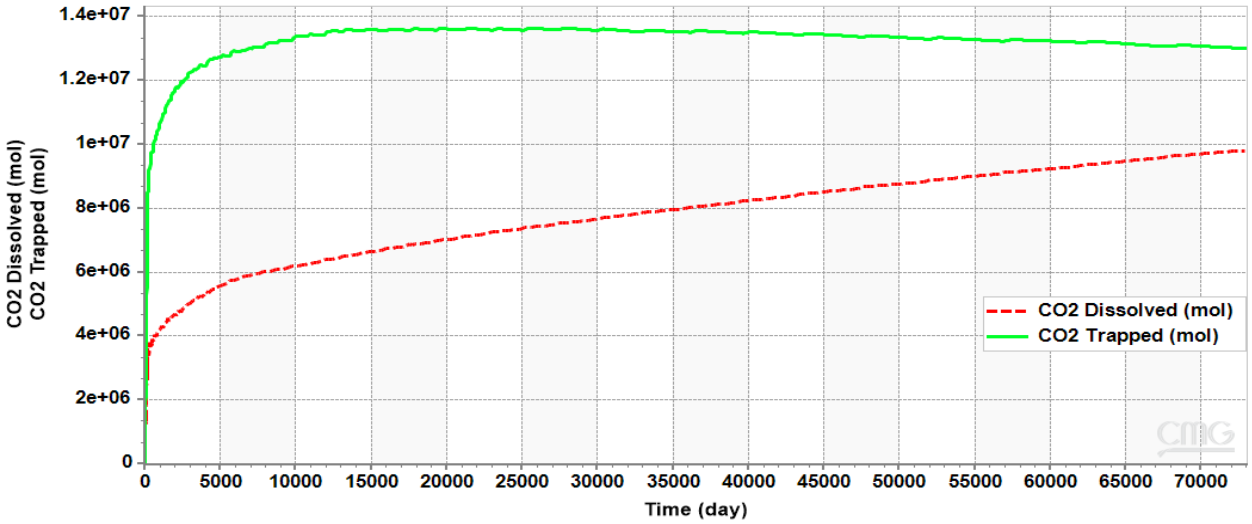

Figure 7. CO_2 dissolved and trapped for 200000ppm water salinity

CO_2 Dissolved and Trapped in 300000ppm Water

Figure 8 shows the CO_2 plume migration in saline aquifer of water salinity 300000ppm.With the CO_2 injector shut-in after 5years and CO_2 plume migration occurring under natural buoyancy during the next 195years, a gas cap of mobile supercritical CO_2 of size 482.2156m was formed at the top of the structure.

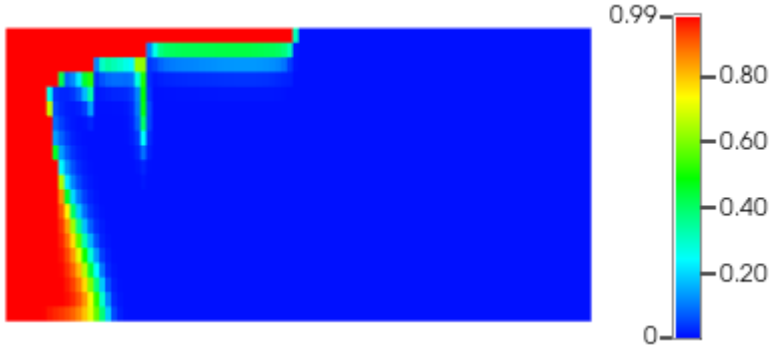

Figure 8. CO_2 spatial distribution for 300000ppm water salinity level

The amount of CO_2 trapped structurally during the injection period and post-injection period for 300000ppm water salinity level is presented in figure 9. 11855227moles of CO_2 was trapped structurally in the injection phase and 15193304 moles for the post injection phase due to the onset of CO_2 solubility trapping. During the injection phase, 2364830.5moles of CO_2 was soluble in water while in the post-injection period, 4788070.5moles of CO_2 was soluble in water.

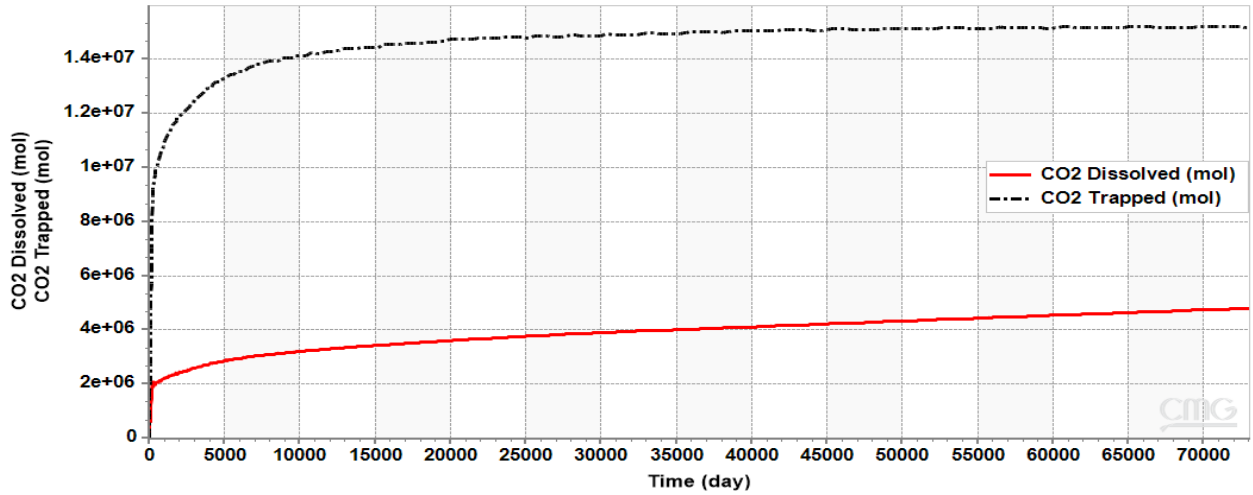

Figure 9. CO_2 trapped and dissolved in water for 300000ppm water salinity level

Comparison of CO_2 Dissolved in Brine and Pure Water

The amount of CO_2 dissolved in brine of different salinities with respect to time is presented in figure 10.The amount of CO_2 dissolved decreases as the brine salinity increases.

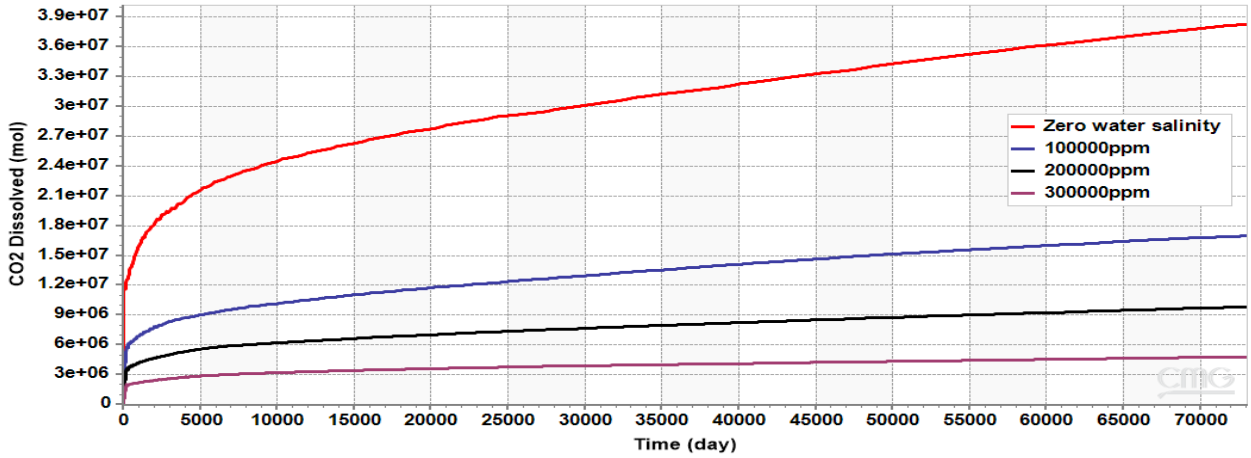

Figure 10. Comparison of the amount of CO_2 dissolved for all water salinity levels

Figure 11 shows a direct comparison of the amount of CO_2 dissolved in pure water and brines of different salinities. There was a decrease in the amount of dissolved CO_2 from 38286492moles to 16974034moles when the water salinity was increased from zero to 100000ppm. For water salinity of 100000ppm, 200000ppm and 300000ppm, the amount of CO_2 dissolved decreases as the water salinity increases. This occurs due to the reduction in gas solubility as the water salinity increases and the formation of a high saturation of mobile CO_2 at the top of the formation. For water salinity levels of 100000ppm, 200000ppm and 300000ppm, result shows that 16974034moles, 9807470moles and 4788070.5moles were solubilised in water.

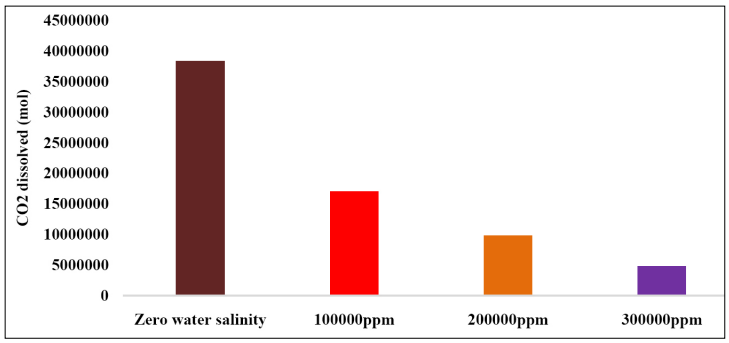

Figure 11. Comparison of CO_2 dissolution for different water salinity levels

Comparison of CO_2 Trapped in Brine and Pure Water

The amount of CO_2 trapped in formation with brine of different salinities with respect to time is shown in figure 12. The results obtained indicated that the amount of CO_2 trapped structurally increases as the water salinity increases because of the reduced CO_2 solubility as a result of high-water salinities.

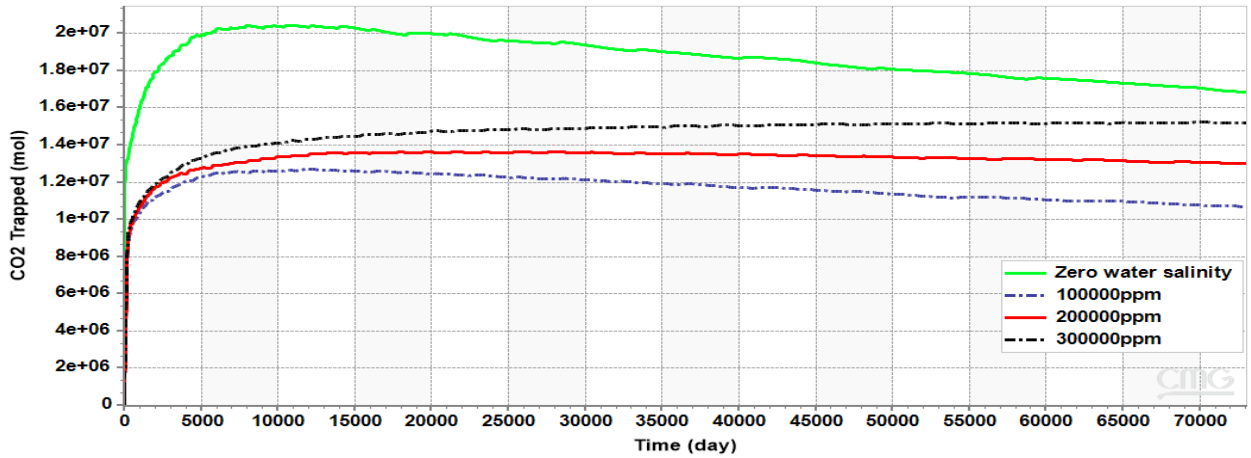

Figure 12. Comparison of the amount of CO_2 trapped for all water salinity levels

Figure 13 shows the amount of CO_2 trapped for zero water salinity level, 100000ppm, 200000ppm and 300000ppm respectively. The results obtained shows an initial decrease in the amount of CO_2 trapped from 16853558moles to 10693296moles when the water salinity was increased from zero to 100000ppm. For water salinity of 100000ppm, 200000ppm and 300000ppm, the amount of CO_2 trapped increases as the water salinity increases. This occurs due to the reduction in gas solubility as the water salinity increases and the formation of a high saturation of mobile CO_2 at the top of the formation. For water salinity levels of 100000ppm, 200000ppm and 300000ppm respectively, result shows that 10693296moles, 13000772moles and 15193304moles were respectively trapped.

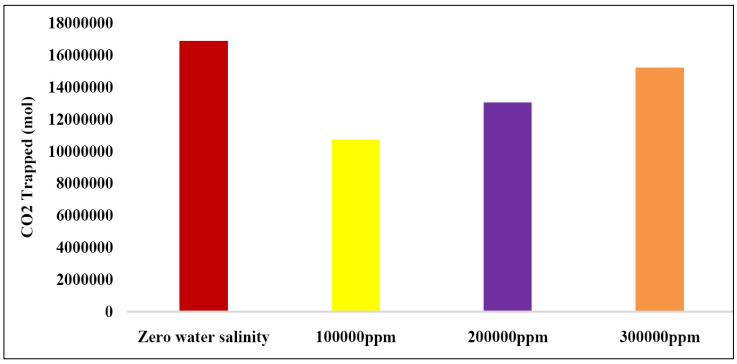

Figure 13. Comparison of CO_2 trapped for different water salinity levels

CONCLUSION

This work evaluates the influence of brine salinity at different concentration on CO_2 dissolution and trapping during sequestration. A simulation based approach was used and sensitivity done for different salinity level and outputs compared with the following conclusions drawn:

i. The amount of CO_2 dissolved decreases with increase in brine salinity concentration.

ii. The amount of CO_2 trapped structurally increases with brine salinity increase.

iii. The gas cap size (length) increases with increase in water salinity concentration

REFERENCES

1. Agartan, E., Trevisan, L., Cihan, A., Birkholzer, J. T., Zhou, Q., and Illangasekare, T. H. (2015). Experimental study on effects of geologic heterogeneity in enhancing dissolution trapping of supercritical CO2. *Water Resources Research, 51*, 1635–1648.

2. Ahmadi, M. A., Pouladi, B., and Barghi, T. (2016). Numerical modeling of CO2 injection scenarios in petroleum reservoirs: Application to CO2 sequestration and EOR. *Journal of Natural Gas Science and Engineering,* 30, 38–49.

3. Ahmadi, P., and Chapoy, A. (2018). CO2 solubility in formation water under sequestration conditions. *Fluid Phase Equilibria,* 463, 80–90.

4. Alkan, H., Cinar, Y., and Ülker, E. (2010). Impact of capillary pressure, salinity and in situ conditions on CO2 injection into saline aquifers. *Transport in Porous Media,* 84(3), 799–819.

5. Al-Khdheeawi, E. A., Vialle S., Barifcani, A., Sarmadivaleh, M., Zhang, Y., and Iglauer, S. (2018). Impact of salinity on CO2 containment security in highly heterogeneous reservoirs. *Greenhouse Gases: Science and Technology,* 8(1), 93–105.

6. Amadichuku N., Kinate B. B., Isidore, E. A., and Epelle, S. I. (2023) The Impact of Relative Permeability Hysteresis on CO2 Sequestration in Saline Aquifer. *Current Trends in Engineering Science,* 3,1026

7. Amarasinghe, W., Fjelde, I., and Guo, Y. (2021). CO2 Dissolution and Convection in Oil at Realistic Reservoir Conditions: A Visualization Study. *Journal of Natural Gas Science and Engineering,* 95, 104113.

8. Chalbaud, C., Robin, M., Lombard, J., Martin, F., Egermann, P., and Bertin, H. (2009). Interfacial tension measurements and wettability evaluation for geological CO2 storage. *Advances in Water Resources*, 32(1), 98–109.

9. De Silva, G., Ranjith, P. G., and Perera, M. (2015). Geochemical aspects of CO2 sequestration in deep saline aquifers: a review. *Fuel,* 155, 128–143.

10. Faisal, T. F., Chevalier, S., and Sassi, M. (2013). Experimental and Numerical Studies of Density Driven Natural Convection in Saturated Porous Media with Application to CO2 Geological Storage. *Energy Procedia,* 37, 5323–5330.

11. Leung, D. Y. C., Caramanna, G., and Maroto-Valer, M. M. (2014). An overview of current status of carbon dioxide capture and storage technologies. *Renewable and Sustainable Energy Reviews*, 39, 426–443.

12. Mathieu, P. (2006). The IPCC special report on carbon dioxide capture and storage. *Proceedings of the 19th International Conference on Efficiency, Cost, Optimization, Simulation and Environmental Impact of Energy Systems*, 1611–1618.

13. Nordbotten, J. M., Celia, M. A., and Bachu, S. (2005). Injection and Storage of CO2 in Deep Saline Aquifers: Analytical Solution for CO2 Plume Evolution During Injection. *Transport in Porous Media*, 58, 339–360.

14. Otheim, T. L., Adam, L., Van Wijk, K., Batzle, M. L., McLing, T., and Podgorney, R. (2011). CO2 sequestration in basalt: carbonate mineralization and fluid substitution. *The Leading Edge,* 30(12), 1354–1359.

15. Shukla, R., Ranjith, P., Haque, A., and Choi, X. (2010). A review of studies on CO2 sequestration and caprock integrity. *Fuel,* 89(10), 2651–2664.

16. Taheri, A., Torsæter, O., Lindeberg, E., Hadia, N. J., Wessel-Berg, D. (2021). Effect of Convective Mixing Process on Storage of CO2 in Saline Aquifers with Layered Permeability. *Advances in Chemical Research,*3, 1–21.

17. Xie, X., and Economides, M. J. (2009). The impact of carbon geological sequestration. *Journal of Natural Gas Science and Engineering*, 1(3), 103–111.

18. Yan, W., Huang, S., and Stenby, E. H. (2011). Measurement and modeling of CO2 solubility in NaCl brine and CO2–saturated NaCl brine density. *International Journal of Greenhouse Gas Control,* 5(6), 1460–1477.

19. Zhao, H., Fedkin, M. V., Dilmore, R. M., and Lvov, S. N. (2015). Carbon dioxide solubility in aqueous solutions of sodium chloride at geological conditions: experimental results at 323.15, 373.15, and 423.15K and 150bar and modeling up to 573.15K and 2000bar. *Geochimica et Cosmochimica Acta,* 149, 165–189.

Citation: Bright Bariakpoa Kinate, Seth Uba Wadike, Godloves Tondie Nonju, Nyelebuchi Amadichuku, "Brine Salinity: A Deciding Factor for Carbondioxide Dissolution and Trapping during Geological Sequestration", Universal Library of Engineering Technology, 2024; 1(1): 41-49. DOI: https://doi.org/10.70315/uloap.ulete.2024.0101006.